INSTITUTE OF PHYSICS PUBLISHING JOURNAL OF PHYSICS: CONDENSED MATTER

J. Phys.: Condens. Matter **13** (2001) 6095–6113 PII: S0953-8984(01)22895-1

The non-hexagonal flux-line lattice in superconductors

Damian P Hampshire

Department of Physics, Superconductivity Group, University of Durham, South Road, Durham DH1 3LE, UK

Received 15 March 2001, in final form 10 May 2001
Published 22 June 2001
Online at stacks.iop.org/JPhysCM/13/6095

Abstract

A generalized form of Ginzburg–Landau theory is proposed which explains the non-hexagonal flux-line lattice found both in metallic and magnetic superconductors without invoking any anisotropic material-dependent properties. The Gibbs energy density postulated for magnetic superconductors (g) is of the form $g(\boldsymbol{B}, T) = \alpha|\psi|^2 + \frac{1}{2}\beta|\psi|^4 + [1/(2m)]|(-\mathrm{i}\hbar\,\boldsymbol{\nabla} - 2e\boldsymbol{A})\psi|^2 + \int(\boldsymbol{B}/\mu_0 - \boldsymbol{M}_{ions}) \cdot \mathrm{d}\boldsymbol{B} - (\boldsymbol{B}/\mu_0 - \boldsymbol{M}_{ions}) \cdot (\mu_0\boldsymbol{M} + \mu_0\boldsymbol{H}_{ext})$ where $\boldsymbol{M}$ is the total local magnetization, $\boldsymbol{M}_{ions}$ is the local magnetization of the magnetic ions and $\boldsymbol{H}_{ext}$ is the externally applied field strength. The macroscopic Gibbs energy density and magnetization close to the upper critical field have been calculated for all possible periodic flux-line lattice structures, for high and low values of the Ginzburg–Landau constant (κ) in both metallic and magnetic superconductors.

The generalized theory is consistent with standard theory for high-κ metallic superconductors. However, for low-κ and/or strongly paramagnetic superconductors for which $(1 + \chi')/2 < \kappa^2 < 3.45(1 + \chi')^2/(1 - \chi')^2$, where χ' is the differential susceptibility of the paramagnetic ions in the normal state, non-hexagonal flux-line lattice structures occur. When the flux-line lattice is non-hexagonal, $(\partial\langle\boldsymbol{M}_{SC}\rangle/\partial\langle\boldsymbol{H}_{ext}\rangle)_{H_{ext}\approx H_{C2}} = (1 - \chi')/(3 + \chi')$. Ferromagnetic and antiferromagnetic superconductivity occur when $\chi' > 1$. Furthermore, increasingly strong paramagnetism coexisting with superconductivity can produce a type I–type II phase transition. Experimental evidence for these phenomena and for a correlation between strong paramagnetism in magnetic superconductors and re-entrant superconductivity is discussed.

1. Introduction

The Ginzburg–Landau (G–L) theory for superconducting materials provides the most widely used framework for describing metallic and magnetic superconductors in magnetic fields [1]. In its original form, it describes the properties of extreme type II metallic superconductors

close to the upper critical field and T_C. Gorkov later showed that for this limited range of materials and phase space, the theory is consistent with microscopic theory [2]. When G–L theory is extended to lower magnetic fields and low-κ materials, broad agreement between theory and experiment remains. It explains the origins of the two classes of superconductor—type I and type II. The magnetic response of superconductors is described qualitatively correctly, including the role of the lower and upper critical fields in type II materials. It also describes the hexagonal flux-line lattice that is commonly found in metallic superconductors in high fields [3]. There is little doubt that G–L theory must include most of the important elements required to describe the properties of superconductors in magnetic fields.

Nevertheless, early magnetic studies on low-κ superconductors (Nb [4], V [5] and Pb alloys [6, 7]) showed a first-order phase transition at the lower critical field which suggested that the flux-line lattice is not always hexagonal [8]. The non-hexagonal flux-line lattice was found in Pb–Tl alloys using Bitter pattern techniques in low magnetic fields [9]. The structure of the flux-line lattice was found to be strongly correlated with its orientation to the crystal structure [7]. Anisotropy in material properties such as the energy gap [10], the elastic properties of the flux-line lattice [11], the Fermi surface [12] and the microscopic electronic and phononic properties [13] were all investigated theoretically to explain non-hexagonal flux-line lattice structures. More recently, there have been intensive neutron scattering studies of magnetic superconductors that show non-hexagonal flux-line lattice structures in high magnetic fields. Square [14–16], rectangular [9] and rhombohedral [14] flux-line lattice structures have all been observed experimentally. Renewed effort has been directed at understanding material-dependent, microscopic properties to explain the non-hexagonal lattice including non-local effects [17], and unconventional symmetries of the order parameter [18, 19]. There is no doubt that the anisotropy of the normal-state electronic and superconducting properties can distort the hexagonal flux-line lattice. However, a different approach is adopted in this paper [20]. Generalized Ginzburg and Landau equations are used to describe the thermodynamic properties of both metallic and magnetic superconductors. It is shown that non-hexagonal lattices can also be explained without introducing any anisotropic material-dependent properties. It is understood that this is a controversial approach, since there is a vast body of theoretical and experimental work in the literature which the scientific community naturally has taken to provide strong support for the validity of the standard G–L equations. However, the formulism outlined in this paper broadly agrees with standard results for high-κ, metallic superconductors. The new properties arise for low-κ and/or strongly paramagnetic superconductors where agreement between standard theory and experimental work is far less secure. Indeed experimental support for the generalized framework proposed is discussed near the end of the paper.

The paper is structured as follows. Section 2 provides the definitions for the field and energy terms used in this paper. Section 3 reviews standard G–L theory and justifies the generalization proposed. In section 4, the results that follow from the general G–L theory are presented both in graphical and analytical form. Calculations of the macroscopic Gibbs energy density and the macroscopic magnetization for both metallic and magnetic superconductors in applied fields close to the upper critical field, for all flux-line lattice structures and any value of κ (recall: κ is the Ginzburg–Landau parameter) are presented. The conditions for non-hexagonal flux-line lattice structures and antiferromagnetic and ferromagnetic superconductivity [20] are provided. Finally, comparison between the theory and experimental data in the literature is made. The generalized theory provides an explanation for the type I–type II phase transition observed in metallic and magnetic superconductors [21–23] and may also explain re-entrant superconductivity in some strongly magnetic superconductors.

2. Definitions of fields and energies for superconductors

There are many different conventions used to define the characteristic fields and energies relevant for the analysis of superconductors. This section outlines the definitions of the symbols used in this paper. An important issue is the distinction between microscopic or local (i.e. intensive) properties and macroscopic (i.e. extensive) properties. It is assumed in this paper that the intensive properties at any point are defined by an average over the local region and that this region is much shorter than any of the characteristic lengths in G–L theory. Macroscopic properties are an average for the entire cylindrical sample.

The symbol used for the local net field is $\boldsymbol{B}$. The local magnetization which by definition is the sum of the magnetic moments within a local volume divided by the local volume is $\boldsymbol{M}$. For magnetic superconductors, the contribution from the magnetic ions ($\boldsymbol{M}_{ions}$) can be separated from that of the supercurrent ($\boldsymbol{M}_{sc}$) where by definition $\boldsymbol{M} = \boldsymbol{M}_{sc} + \boldsymbol{M}_{ions}$. Following the usual definitions, the local magnetic field strength $\boldsymbol{H}$ is given by $\boldsymbol{H} = \boldsymbol{B}/\mu_0 - \boldsymbol{M}$ and the local magnetic vector potential $\boldsymbol{A}$ by $\boldsymbol{B} = \boldsymbol{\nabla} \times \boldsymbol{A}$. The macroscopic equivalent parameters are described using angular brackets, so by definition $\langle \boldsymbol{B} \rangle = \int \boldsymbol{B}\, \mathrm{d}V$ and the volume integral is for the entire system (i.e. all space). This integral produces characteristic values of the relevant variable for the whole material. Use of lower case letters for energy terms will denote so-called specific properties (i.e. energy per unit volume). As with field terms, angular brackets are used to distinguish energies that are macroscopic rather than local.

A self-consistent set of thermodynamic functions can be used to find equilibrium properties. We first follow the formulism outlined by de Gennes and others [24–26]. Consider a set of coils that produce an applied field strength, $\boldsymbol{H}_{ext}$, and contain a magnetic material of any type. If the current in the coils is changed, the work done by the external currents ($\boldsymbol{J}_{ext}$) in a time δt is by definition the change in the Helmholtz energy (δF) where $F = U - TS$. Using Maxwell's equations $\boldsymbol{\nabla} \times \boldsymbol{E} = -\mathrm{d}\boldsymbol{B}/\mathrm{d}t$ and $\boldsymbol{\nabla} \times \boldsymbol{H} = \boldsymbol{J}_{ext}$ and the vector identity $\boldsymbol{\nabla} \cdot (\boldsymbol{H} \times \boldsymbol{E}) = \boldsymbol{H} \cdot (\boldsymbol{\nabla} \times \boldsymbol{E}) - \boldsymbol{E} \cdot (\boldsymbol{\nabla} \times \boldsymbol{H})$, this can be written as

$$\partial F = -\langle \boldsymbol{E} \cdot \boldsymbol{J}_{ext} \rangle\, \partial t = \langle \boldsymbol{H} \cdot \mathrm{d}\boldsymbol{B} \rangle. \tag{1}$$

This expression for the Helmholtz energy fully accounts for a spatial variation in $\boldsymbol{H}$ and $\boldsymbol{B}$. One can construct the Gibbs energy by adding a term which can be called the Zeeman term [27] so that

$$G = F - \langle \boldsymbol{B} \cdot \boldsymbol{H} \rangle. \tag{2}$$

Using $\boldsymbol{\nabla} \cdot \boldsymbol{B} = 0$ and $\boldsymbol{B} = \boldsymbol{\nabla} \times \boldsymbol{A}$, and integrating by parts, it can be shown that

$$\mathrm{d}G = -\langle \boldsymbol{B} \cdot \mathrm{d}\boldsymbol{H} \rangle = -\langle \boldsymbol{A} \cdot \partial \boldsymbol{J}_{ext} \rangle. \tag{3}$$

Thus $\partial G = 0$ when T and the externally applied field are fixed.

One can also separate the Helmholtz energy associated with the magnetic material ($F_{Material}$) from that of the coils (F_{Coils}). Equation (1) can be rewritten as

$$\partial F = \mu_0 \langle \boldsymbol{H} \cdot \mathrm{d}\boldsymbol{H} \rangle + \mu_0 \langle \boldsymbol{H} \cdot \mathrm{d}\boldsymbol{M} \rangle = \partial F_{Material} + \partial F_{Coils}. \tag{4}$$

Hence one can construct a Gibbs energy for the material ($G_{Material}$) of the form

$$G_{Material} = F_{Material} - \mu_0 \langle \boldsymbol{H} \cdot \boldsymbol{M} \rangle \tag{5}$$

where again $\partial G_{Material} = 0$ when T and the externally applied field are fixed.

Following much of the literature, the analysis in this paper is limited to an isotropic cylindrical superconductor of unit volume with the applied field parallel to the axis of the cylinder. This reduces the analysis to two dimensions and eliminates the need to introduce volume terms or demagnetization factors. Standard notation is used so that

the superconductivity is destroyed when the applied field strength is $\boldsymbol{H}_{C2}$. For magnetic superconductors the upper critical field ($\boldsymbol{B}_{C2}$) is given by $\boldsymbol{B}_{C2} = \mu_0(1+\chi')\boldsymbol{H}_{C2}$ where χ' is the differential susceptibility of the paramagnetic ions. For metallic superconductors $\chi' = 0$.

3. Ginzburg–Landau theory for metallic and magnetic superconductors

Ginzburg and Landau proposed a local Helmholtz energy density (f) for a metallic superconductor of the form [1]

$$f = \alpha\,|\psi|^2 + \frac{1}{2}\beta\,|\psi|^4 + \frac{1}{2m}\,|(-\mathrm{i}\hbar\,\boldsymbol{\nabla} - 2e\boldsymbol{A})\psi|^2 + \int \boldsymbol{H}_{G-L}\cdot \mathrm{d}\boldsymbol{B} \tag{6}$$

where α and β are constants and ψ is the wavefunction. The integral is known as the field energy-density term where $\boldsymbol{H}_{G-L} = \boldsymbol{B}/\mu_0$ for metallic superconductors and $\boldsymbol{H}_{G-L} = \boldsymbol{B}/\mu_0 - \boldsymbol{M}_{ions}$ for magnetic superconductors where $\boldsymbol{M}_{ions}$ is the magnetization of the ions [1, 3, 24, 28, 29]. The primary support for the G–L equations as they are usually constructed comes from experiment and theory for high-κ materials. We suggest that the confirmation of their validity of the equations for low-κ and/or strongly magnetic superconductors is not provided by experiment.

In constructing the Gibbs energy density from this Helmholtz functional, one must identify the minimum volume which may be considered to reach a local equilibrium. For the magnetic systems considered in section 2, any region of interest reaching equilibrium is larger than the length scale on which currents flow that produce the magnetic moments. The magnetic moments produce flux that is completely contained within the region of interest. This assumption is not generally true for superconductors [30]. For type II superconductors, although the wavefunction varies on the scale of the coherence length (ξ), the length scale over which energy changes occur when the supercurrent density changes is macroscopic. For simplicity we assume in this paper that local equilibrium is reached on a length scale that is much smaller that any of the other characteristic length scales for the superconductivity but larger than atomic lengths. The moments (i.e. circulating supercurrent density) can be considered to intersect the region of interest and produce flux that is both inside and outside of it[1]. Equally, supercurrents outside the region of interest produce flux within it. We retain the Helmholtz energy density postulated by Ginzburg and Landau, since it follows from the conservation of energy for the macroscopic system if it is interpreted as the work done by both external field and superelectrons. It also has the necessary property that changes in f do not depend on the source of the change in the magnetic field at the point of interest (i.e. f depends on $\boldsymbol{B}$). We use a physical argument to find the Zeeman term which added to the Helmholtz energy density gives the Gibbs energy density—which by definition has a minimum value in equilibrium. The necessity for a Zeeman term is well established in deriving the properties of superconducting thin films [8]. In general it accounts for the increase in entropy that follows from the moment dropping to a lower energy level (or in classical terms rotating into the direction of the applied field). We assume that there is a field contribution to the region of interest both from the external field and from the supercurrents and that there is a contribution to the moments inside the region of interest from both the supercurrent and the magnetic ions. This gives a Zeeman term of the form $(\boldsymbol{B}/\mu_0 - \boldsymbol{M}_{ions})\cdot\boldsymbol{M}$, where $\boldsymbol{M}$ is the total magnetization produced by the superelectrons and the magnetic ions at any point of interest. The term is consistent with that required to describe metallic thin films [8]. We also add in a term $\boldsymbol{H}_{ext}$ which changes the zero-Gibbs-energy-density condition and ensures that if the

[1] In this context it is useful to think of a local definition of magnetic moment where $\int \boldsymbol{M}\,\mathrm{d}V = \frac{1}{2}\int \boldsymbol{r}\times\boldsymbol{J}\,\mathrm{d}V$ where $\boldsymbol{r}$ is the radius vector [25, 26].

material is not superconducting, the properties of the magnetic ions are properly described. The G–L equations are unaffected by adding $\boldsymbol{H}_{ext}$. Hence we postulate that the Gibbs energy density is of the form

$$g(\boldsymbol{B}, T) = \alpha\,|\psi|^2 + \frac{1}{2}\beta\,|\psi|^4 + \frac{1}{2m}\,|(-\mathrm{i}\hbar\,\boldsymbol{\nabla} - 2e\boldsymbol{A})\psi|^2 + \int\left(\frac{\boldsymbol{B}}{\mu_0} - \boldsymbol{M}_{ions}\right)\cdot \mathrm{d}\boldsymbol{B} - \left(\frac{\boldsymbol{B}}{\mu_0} - \boldsymbol{M}_{ions}\right)\cdot(\mu_0\boldsymbol{M} + \mu_0\boldsymbol{H}_{ext}). \tag{7}$$

Equilibrium properties are found from solutions which self-consistently minimize g. We note that in the standard literature, the same G–L equations follow when minimizing either the Helmholtz energy density or the Gibbs energy density, so for bulk materials the two energy-density terms are often used interchangeably [28, 31]. In the generalized formulism proposed, g (rather than f) must be minimized to find equilibrium properties.

This paper considers magnetic superconductors which have been a long-standing and interesting issue [32]. Much of the early experimental work in this area was compromised by uncertainty as to whether the superconductivity and the magnetic ordering really coexisted in the same part of the material or whether the material in fact consisted of two separate phases. However, there are a number of different classes of materials in which it is now generally believed that the superelectrons and the ions responsible for the magnetic ordering coexist within the unit cell [32–34] but are spatially separated. Hence the exchange interaction between the superelectrons and the magnetic ions which often prevents superconductivity occurring [35] is negligible. The dominant interaction is dipolar. This interaction produces low ordering temperatures of order 1 K (cf. section 6). The simplest magnetic superconductors are considered [29] where the crystal structure ensures that although the interaction between the magnetic ions themselves can be dipolar and/or exchange driven, the superelectrons and the magnetic ions are completely spatially separated [33, 34].

4. Equilibrium properties of superconductors

An important question that arises is whether the Gibbs energy-density functional proposed is in principle solvable for both metallic and magnetic superconductors. The G–L equations for metallic superconductors have two unknowns, the local wavefunction and the local value of magnetization from the supercurrent. They completely specify the magnetic properties of the superconductor. The spatial variation and magnitude of these two unknowns are found as a function of the local net field by simultaneously solving the two G–L equations. Macroscopic properties can then be calculated self-consistently in terms of the externally applied field. At first sight, when magnetic superconductors are described using the functional (and indeed equivalent functionals in the literature), it appears problematic since the functional includes a third unknown variable $\boldsymbol{M}_{ions}$. However, when the superelectrons are spatially separated from the magnetic ions, $\boldsymbol{M}_{ions}$ is determined only by the local net field, independently of whether the material is in the superconducting or the normal state. Hence the normal-state properties of the magnetic ions provide a third equation or equivalently a constraint on $\boldsymbol{M}_{ions}$ in terms of $\boldsymbol{B}$. We conclude that in conjunction with this constraint, the functional proposed can be solved quite generally to give the values of the local wavefunction and $\boldsymbol{M}_{sc}$ (and $\boldsymbol{M}_{ions}$) in terms of $\boldsymbol{B}$.

In Abrikosov's original work, he found a periodic structure for the flux-line lattice [3]. Kleiner *et al* subsequently found that the equilibrium state was the hexagonal flux-line lattice [36]. In this section, we follow broadly the mathematical approach of Abrikosov/Kleiner to find equilibrium properties as outlined in the excellent text by Tilley and Tilley [28].

4.1. Metallic superconductors

First, consider metallic superconductors. Minimizing equation (7) with respect to the wavefunction gives the first G–L equation:

$$\alpha\psi + \beta|\psi|^2\psi + \frac{1}{2m_e}(-\mathrm{i}\hbar\,\boldsymbol{\nabla} - 2e\boldsymbol{A})^2\psi = 0. \tag{8}$$

The linearized wavefunction (ψ_L), first proposed by Abrikosov [3], is a solution to the first G–L equation with the term in β set to zero. It is of the form

$$\psi_L(x, y) = \sum_{n=-\infty}^{\infty} C_n \exp(\mathrm{i}nky)\exp\left[-\frac{(x - x_n)^2}{2\xi^2(T)}\right] \tag{9}$$

where one can prove [28]

$$\frac{x_n}{nk} = \xi^2(T)\frac{\hbar^2}{2m|\alpha|} \tag{10}$$

and

$$\mu_0 H_{C2} = \frac{\varphi_0}{2\pi\xi^2(T)} \tag{11}$$

where C_n are constants, ξ is the coherence length and the upper critical field $\boldsymbol{B}_{C2} = \mu_0\boldsymbol{H}_{C2}$ [28]. The values of k and C_n are chosen to describe a periodic array of vortices. Abrikosov found a mathematical identity for this wavefunction of the form [3]

$$\frac{e\hbar}{m_e}\boldsymbol{\nabla}\times(|\psi_L|^2\hat{\boldsymbol{k}}) = \frac{\mathrm{i}e\hbar}{m_e}(\psi_L^*\,\boldsymbol{\nabla}\psi_L - \psi_L\,\boldsymbol{\nabla}\psi_L^*) + \frac{4e^2}{m_e}\psi_L^*\psi_L\boldsymbol{A}_{C2} \tag{12}$$

where $\boldsymbol{B}_{C2}$ is related to $\boldsymbol{A}_{C2}$ by

$$\boldsymbol{B}_{C2} = \boldsymbol{\nabla}\times\boldsymbol{A}_{C2} = \frac{\phi_0}{2\pi\xi^2}\hat{\boldsymbol{k}} \tag{13}$$

and φ_0 is the fundamental flux quantum. Abrikosov's [3] constant is required in this paper; it is defined by

$$\beta_A = \frac{\langle|\psi_L|^4\rangle}{\langle|\psi_L|^2\rangle^2}. \tag{14}$$

The constant β_A has a value of 1.16 for the hexagonal structure, 1.18 for the square structure and is higher for rectangular and rhombohedral structures of high aspect ratio [36].

The second G–L equation is obtained by minimizing the Gibbs energy density with respect to the magnetic vector potential. We assume that self-consistent solutions can be found for $\boldsymbol{M}_{SC}$ and ψ, if $\boldsymbol{M}_{SC}$ is of the form

$$\boldsymbol{M}_{SC} = -\frac{(\boldsymbol{B}_{C2} - \boldsymbol{B})}{\mu_0}S \tag{15}$$

where S is independent of magnetic field and temperature. Equation (15) necessarily ensures that when $\boldsymbol{B} = \boldsymbol{B}_{C2}$, $\boldsymbol{M}_{SC} = 0$. It is important to note that when relating $\boldsymbol{M}_{SC}$ to $\boldsymbol{B}$, one is averaging out the detailed structure of the moments. This averaging is an important issue when calculating the structure of fluxons. Nevertheless we make this assumption to ensure that to first order, all required terms in g are explicitly included. The function $+\int(\boldsymbol{B}/\mu_0 - \boldsymbol{M}_{ions})\cdot\mathrm{d}\boldsymbol{B} - (\boldsymbol{B}/\mu_0 - \boldsymbol{M}_{ions})\cdot(\mu_0\boldsymbol{M} + \mu_0\boldsymbol{H}_{ext})$ can be expressed as a parabolic function of $\boldsymbol{B}$. We define P as the scalar coefficient of the term in $\boldsymbol{B}^2/2\mu_0$ in the parabolic function. Hence the second generalized G–L equation can be written in the form

$$P\,\boldsymbol{\nabla}\times\frac{\boldsymbol{B}}{\mu_0} = -\frac{\mathrm{i}e\hbar}{m_e}(\psi^*\,\boldsymbol{\nabla}\psi - \psi\,\boldsymbol{\nabla}\psi^*) - \frac{4e^2}{m_e}\psi^*\psi\boldsymbol{A} \tag{16}$$

where

$$P = 1 - 2S. \tag{17}$$

For metallic superconductors, $\boldsymbol{\nabla} \times \boldsymbol{B} = \mu_0 \boldsymbol{\nabla} \times \boldsymbol{M}_{SC}$. Comparing the second G–L equation with the Abrikosov identity gives for $\boldsymbol{B} \approx \boldsymbol{B}_{C2}$

$$\boldsymbol{M}_{SC} = -\frac{e\hbar|\psi_L|^2}{P_r m_e}\hat{\boldsymbol{k}}. \tag{18}$$

There are a number of techniques for finding $|\psi_L|^2$. Close to the upper critical field, we assume that self-consistent solutions to the G–L equations can be found of the form [28]

$$\boldsymbol{A} = \boldsymbol{A}_{C2} + \boldsymbol{A}_1 \tag{19}$$

and

$$\psi = \psi_L. \tag{20}$$

Taking the non-linear first G–L equation, multiplying by ψ_L^* and integrating over all space, and then using the Abrikosov identity gives for $\boldsymbol{B} \approx \boldsymbol{B}_{C2}$ [20, 28]

$$\left\langle \left(\frac{e\hbar}{m_e} \boldsymbol{A}_1 \cdot \boldsymbol{\nabla} \times (|\psi_L|^2 \hat{\boldsymbol{k}}) + \beta |\psi_L|^4 \right) \right\rangle = 0. \tag{21}$$

Using equations (18) and (19), equation (21) can be written as

$$\left\langle (-P\boldsymbol{M}_{SC} \cdot (\boldsymbol{B} - \boldsymbol{B}_{C2}) + \beta |\psi_L|^4) \right\rangle = 0 \tag{22}$$

or equivalently

$$\left\langle \left(\frac{e\hbar}{m_e} |\psi_L|^2 (B - B_{C2}) + \beta |\psi_L|^4 \right) \right\rangle = 0. \tag{23}$$

Hence $\langle |\psi_L|^2 \rangle$ is of the form

$$\left\langle |\psi_L|^2 \right\rangle = \frac{m_e}{e\hbar\mu_0} \frac{\langle (B_{C2} - B) \rangle}{2\kappa^2 \beta_A} \tag{24}$$

where the volume integrals for terms of the form $(B_{C2} - B)$ are taken over the volume of the superconductor alone and the G–L parameter (κ) is defined by [28]

$$\kappa^2 = \frac{m_e^2 \beta}{2\mu_0 e^2 \hbar}. \tag{25}$$

Substituting equation (24) into the volumetric integral of equation (18) gives

$$\langle \boldsymbol{M}_{SC} \rangle = -\frac{\langle (\boldsymbol{B}_{C2} - \boldsymbol{B}) \rangle}{\mu_0 \, 2\kappa^2 P \beta_A}. \tag{26}$$

Comparing equation (26) to the volumetric integral of equation (15) gives

$$1 = 2\kappa^2 P S \beta_A. \tag{27}$$

Equations (17) and (27) lead to a quadratic equation which has the solutions

$$S = \frac{1 \pm \sqrt{1 - 4/(\beta_A \kappa^2)}}{4}. \tag{28}$$

Hence once β_A is known for the equilibrium structure, equation (28) gives S and hence the local and the macroscopic magnetization. Given that the macroscopic magnetization has been calculated, the structure of the flux-line lattice (or equivalently β_A) in the equilibrium state can be calculated from finding the minimum in the Gibbs energy for the entire material. From the

definition of the Gibbs energy (or macroscopic Gibbs energy density) written in terms of $\boldsymbol{H}$ (cf. equation (5)), one has

$$G_{SC}(H) - G_N(H) = -\mu_0 \int \langle \boldsymbol{M}_{SC} \rangle \cdot \mathrm{d}\boldsymbol{H}. \tag{29}$$

Rewriting $\langle \boldsymbol{M}_{SC} \rangle$ in terms of $\boldsymbol{H}$ gives

$$\langle \boldsymbol{M}_{SC} \rangle = -\frac{\langle (\boldsymbol{B}_{C2} - \boldsymbol{B}) \rangle}{\mu_0} S = -\langle (\boldsymbol{H}_{C2} - \boldsymbol{H}) \rangle \frac{S}{(1-S)}. \tag{30}$$

The difference between the Gibbs energy in the superconducting state ($G_{SC}(H)$) and the normal state ($G_N(H)$), equal to that at $H = H_{C2}$, is

$$G_{SC}(H) - G_N(H) = -\frac{\mu_0 \langle (H_{C2} - H)^2 \rangle}{2} \frac{S}{(1-S)}. \tag{31}$$

For a cylindrical sample, one can replace H by H_{ext}. From equations (28) and (31), for any value of κ, the Gibbs energy can be calculated for any value of β_A (i.e. any periodic flux-line lattice structure). Therefore the values of S and β_A that give the minimum value of the Gibbs energy can be determined. The parameter β_A determines the structure of the flux-line lattice through equation (14) and S gives the macroscopic magnetization through equation (30).

4.2. Magnetic superconductors

The properties of the magnetic ions are described using the normal-state relation:

$$\boldsymbol{M}_{ions} = \chi' \boldsymbol{H} = \frac{\chi' \boldsymbol{B}}{\mu_0 (1 + \chi')} \tag{32}$$

where the bulk differential susceptibility is χ'. Self-consistent solutions for $\boldsymbol{M}_{SC}$ can be found when it is expressed in the form

$$\boldsymbol{M}_{SC} = -\frac{1}{(1+\chi')} \frac{(\boldsymbol{B}_{C2} - \boldsymbol{B})}{\mu_0} S_M \tag{33}$$

where S_M is a function of χ', κ and β_A. The second G–L equation for magnetic superconductors is of the form

$$P_M \boldsymbol{\nabla} \times \frac{\boldsymbol{B}}{\mu_0} = P_M (1+\chi') \boldsymbol{\nabla} \times \boldsymbol{M}_{SC} = -\frac{\mathrm{i}e\hbar}{m_e} (\psi^* \boldsymbol{\nabla} \psi - \psi \boldsymbol{\nabla} \psi^*) - \frac{4e^2}{m_e} \psi^* \psi \boldsymbol{A} \tag{34}$$

where P_M is defined again as the coefficient of $\boldsymbol{B}^2/2\mu_0$ in the function $+\int (\boldsymbol{B}/\mu_0 - \boldsymbol{M}_{ions}) \cdot \mathrm{d}\boldsymbol{B} - (\boldsymbol{B}/\mu_0 - \boldsymbol{M}_{ions}) \cdot (\mu_0 \boldsymbol{M} + \mu_0 \boldsymbol{H}_{ext})$. For magnetic superconductors, equation (8) remains valid. Given that

$$\begin{aligned} &\int (\boldsymbol{B} - \boldsymbol{M}_{ions}) \cdot \mathrm{d}\boldsymbol{B} - (\boldsymbol{B} - \boldsymbol{M}_{ions}) \cdot (\mu_0 \boldsymbol{M} + \mu_0 \boldsymbol{H}_{ext}) \\ &\quad = \frac{1}{\mu_0} \int \left(\boldsymbol{B} - \frac{\chi' \boldsymbol{B}}{1+\chi'} \right) \cdot \mathrm{d}\boldsymbol{B} \\ &\quad\quad - \frac{1}{\mu_0} \left(\boldsymbol{B} - \frac{\chi' \boldsymbol{B}}{1+\chi'} \right) \cdot \left(\frac{\chi' \boldsymbol{B}}{1+\chi'} - \frac{(\boldsymbol{B}_{C2} - \boldsymbol{B}) S_M}{1+\chi'} + \mu_0 \boldsymbol{H}_{ext} \right). \end{aligned} \tag{35}$$

For magnetic superconductors, P_M is given by

$$P_M = \frac{(1 - \chi' - 2S_M)}{(1+\chi')^2}. \tag{36}$$

Equation (27) still holds, and leads to a quadratic equation for S_M which has the solutions

$$S_M = \frac{(1-\chi')}{4}\left(1 \pm \sqrt{1 - \frac{4(1+\chi')^2}{\beta_A \kappa^2 (1-\chi')^2}}\right). \tag{37}$$

We can again consider the macroscopic Gibbs energy written in terms of $\boldsymbol{H}$:

$$G_{SC}(H) - G_N(H) = -\frac{1}{(1+\chi')}\frac{\mu_0 \langle (H_{C2} - H)^2 \rangle S_M}{2(1-S_M)} \tag{38}$$

since

$$\langle \boldsymbol{M}_{SC} \rangle = -\frac{1}{(1+\chi')}\frac{\langle (\boldsymbol{B}_{C2} - \boldsymbol{B}) \rangle}{\mu_0} S_M = -\langle (\boldsymbol{H}_{C2} - \boldsymbol{H}) \rangle \frac{S_M}{(1-S_M)}. \tag{39}$$

For any given values of κ and χ', equations (37) and (38) can be used to determine the value of β_A which gives the minimum Gibbs energy (i.e. when $\beta_A = \beta_A(\mathrm{Max})$) and hence the equilibrium properties. Note that when a material is superconducting, $\langle \boldsymbol{M}_{ions} \rangle$ is changed from its equivalent normal-state value. The difference in the total magnetic moment produced by superconductivity from what would occur in the normal state is $(1+\chi')\langle \boldsymbol{M}_{sc} \rangle$.

5. Graphical and analytic solutions

In principle, equations (28) and (37) provide two solutions of S and S_M for given values of κ, β_A and χ'. However, the positive root is discarded since it leads to $\beta_A \to \infty$ which implies macroscopic regions in the Meissner state. Although the Meissner state is a solution to the two G–L equations, it is not a minimum of the Gibbs energy density close to the upper critical field (except for $\kappa \leqslant 1/\sqrt{2}$). Hence for metallic superconductors S is of the form

$$S = \frac{1 - \sqrt{1 - 4/(\beta_A \kappa^2)}}{4}. \tag{40}$$

Only values of β_A greater than 1.16 are considered, since Kleiner *et al* [36] have shown that this is the lowest possible value of β_A ($\beta_A(\mathrm{hex}) = 1.16$). Comparing equations (31) and (40), the Gibbs energy is minimized when S is a maximum subject to the constraint that S is real so $\kappa^2 \beta_A / 2 \geqslant 1$.

5.1. Metallic superconductors

At values of κ above 1.86, the minimum value of the Gibbs energy occurs when β_A is 1.16, so the structure of the flux-line lattice is hexagonal. As κ decreases below 1.86, higher values of β_A are required to meet the constraint that S is real and hence find the minimum (real) Gibbs energy. Therefore non-hexagonal structures are the most stable. Hence the value of β_A for the lowest energy state (defined as $\beta_A(\mathrm{Max})$) and values of S can be determined for any value of κ from equations (28) and (31). Using the condition that in the Meissner state $\langle |\psi_L|^2 \rangle = |\alpha|/\beta$, it can be shown that materials are type I when $\kappa \leqslant 1/\sqrt{2}$ [29]. In figure 1, values of the dimensionless variables $\beta_A(\mathrm{Max})$, S, $S/(1-S)$ and P are shown as functions of the G–L parameter (κ), for metallic superconductors in equilibrium. There is agreement in the high-κ limit with the Abrikosov result (i.e. $(\partial \langle \boldsymbol{M}_{SC} \rangle / \partial \langle \boldsymbol{H} \rangle)_{H \approx H_{C2}} = 1/[(2\kappa^2 - 1)\beta_A]$) since $S_{(\kappa \to \infty)} = 1/2\kappa^2 \beta_A(\mathrm{hex})$ (cf. equations (30) and (40)).

The solutions can be described analytically. For $\kappa^2 > 4/\beta_A(\mathrm{hex})$, the hexagonal structure is found for the flux-line lattice, $\beta_A = \beta_A(\mathrm{hex}) = 1.16$, and equations (28), (30) and (31)

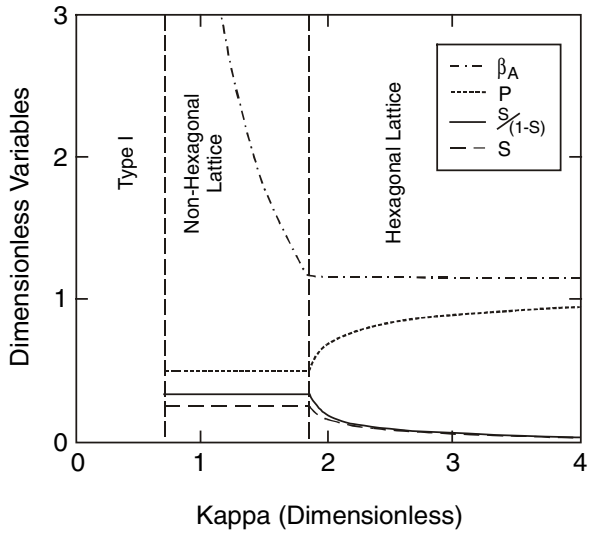

Figure 1. Values of the dimensionless variables $\beta_A(\mathrm{Max})$, S, $S/(1-S)$ and P as functions of the Ginzburg–Landau parameter (κ) for metallic superconductors in equilibrium. When $\kappa < 1/\sqrt{2}$, there is type I behaviour. For $1/\sqrt{2} < \kappa < 1.86$, there is type II behaviour with a non-hexagonal flux-line lattice. For $\kappa > 1.86$, there is type II behaviour with a hexagonal flux-line lattice.

give equilibrium solutions. When $1/2 \leqslant \kappa^2 \leqslant 4/\beta_A(\mathrm{hex})$, (i.e. $0.71 \leqslant \kappa \leqslant 1.86$), the non-hexagonal structure is found for the flux-line lattice where

$$\beta_A(\mathrm{Max}) = 4/\kappa^2 \tag{41}$$

$$S = \frac{1}{4} \tag{42}$$

$$\langle \boldsymbol{M}_{SC} \rangle = -\frac{\langle (\boldsymbol{H}_{C2} - \boldsymbol{H}) \rangle}{3} \tag{43}$$

$$G_{SC} - G_N = -\frac{\mu_0 \langle (H_{C2} - H)^2 \rangle}{6}. \tag{44}$$

Note that (unlike in standard G–L theory) the macroscopic magnetization (equation (43)) and the Gibbs energy (equation (44)) are independent of κ for non-hexagonal flux-line lattice structures.

5.2. Magnetic superconductors

For magnetic superconductors when $\kappa^2 > 4(1+\chi')^2/\beta_A(\mathrm{hex})(1-\chi')^2$, hexagonal structures of the flux-line lattice occur and $\beta_A = \beta_A(\mathrm{hex}) = 1.16$. Equations (41), (43) and (44) give equilibrium properties. The non-hexagonal structures occur when

$$\frac{(1+\chi')}{2} < \kappa^2 < \frac{4(1+\chi')^2}{1.16(1-\chi')^2}$$

(i.e. $(1+\chi')/\sqrt{2} < \kappa < |1.86(1+\chi')/(1-\chi')|$) and one has

$$\beta_A(\mathrm{Max}) = \frac{4(1+\chi')^2}{\kappa^2(1-\chi')^2} \tag{45}$$

$$S = \frac{(1-\chi')}{4} \tag{46}$$

$$\langle \boldsymbol{M}_{SC} \rangle = -\frac{(1-\chi')\langle (\boldsymbol{H}_{C2} - \boldsymbol{H}) \rangle}{(3+\chi')} \tag{47}$$

$$G_{SC} - G_N = \frac{-\mu_0(1-\chi')\left\langle (H_{C2} - H)^2 \right\rangle}{2(3+\chi')}. \tag{48}$$

As with metallic superconductors, the condition for type I behaviour can be derived using the result that in the Meissner state $\langle |\psi_L|^2 \rangle = |\alpha|/\beta$. This gives [29]

$$\kappa^2 \leqslant \frac{(1+\chi')}{2} \tag{49}$$

Graphical solutions for a superconductor with $\kappa = 4$ as a function of susceptibility are shown in figure 2. The values of β_A(Max), S, $S/(1-S)$ and P_M are shown. β_A(Max) determines the structure of the flux-line lattice and shows that although a metallic superconductor (i.e. $\chi' = 0$) with $\kappa = 4$ has a hexagonal structure, as the differential susceptibility increases the structure becomes non-hexagonal when $\chi' \cong 1$ and becomes hexagonal again as χ' increases yet further. The values of S and $S/(1-S)$ change sign at $\chi' = 1$, consistent with the superelectrons producing a diamagnetic response for $\chi' < 1$ and a positive magnetization contribution (ferromagnetic superconductivity) for $\chi' > 1$ [20]. P_M also changes sign at $\chi' = 1$. These sign changes occur for all materials regardless of their κ-value. Since the second Ginzburg–Landau equation leads to the London equation, one can derive a low-field wave equation for the superconductor which shows that when P_M is positive one expects the Meissner state in low fields and when P_M is negative one expects fluxons and antifluxons in the bulk of the material—antiferromagnetic superconductivity [20]. Ferromagnetic and

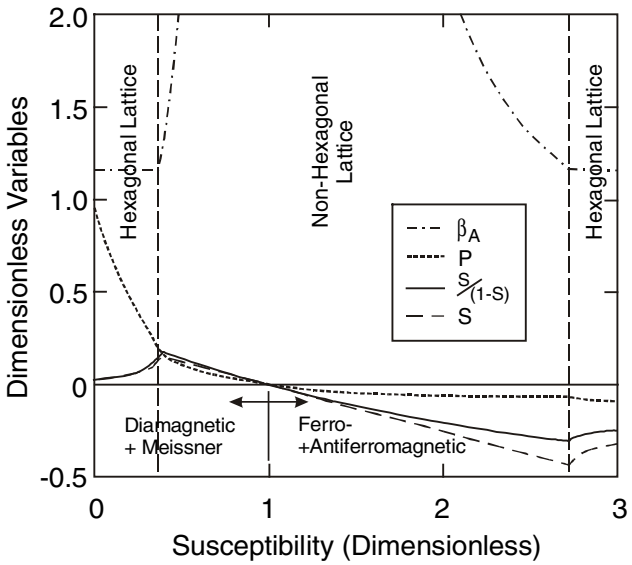

Figure 2. Values of the dimensionless variables β_A(Max), S_M, $S_M/(1-S_M)$ and P_M for a magnetic superconductor where $\kappa = 4$, as functions of the differential susceptibility of the material in the normal state. The boundaries, relevant for high magnetic fields, at which the flux-line lattice changes from hexagonal to non-hexagonal are shown. For $\chi' < 1$, the macroscopic magnetization is diamagnetic in high magnetic fields and the Meissner state in low magnetic fields. For $\chi' > 1$, the equivalent states are ferromagnetic and antiferromagnetic. Not shown (discussed in the text): when $\chi' \cong 1$, β_A(Max) $\to \infty$ and one may expect type I-like behaviour; when $\chi' > 2\kappa^2 - 1$ the material becomes an antiferromagnetic superconductor.

antiferromagnetic superconductivity can be considered very simply in the high-κ limit when $S \ll 1$, since when $\boldsymbol{B} \approx \boldsymbol{B}_{C2}$, $\langle \boldsymbol{M}_{SC} \rangle$ is

$$\langle \boldsymbol{M}_{SC} \rangle = -\frac{(1+\chi')^2}{(1-\chi')} \frac{\langle (\boldsymbol{H}_{C2} - \boldsymbol{H}) \rangle}{2\kappa^2 \beta_A} \tag{50}$$

which clearly shows the change in sign about $\chi' = 1$. Equally in the high-κ limit when $S_M \ll 1$, $P_M = (1-\chi')/(1+\chi')^2$ and equation (34) leads to a generalized London equation and a wave equation of the form [20]

$$\nabla^2 \boldsymbol{B} = \frac{(1+\chi')^2}{(1-\chi')} \frac{\boldsymbol{B}}{\lambda^2} \tag{51}$$

where one uses the usual approximation $\lambda^2 = m/4e^2\mu_0\psi^*\psi$. When $\chi' < 1$, one finds exponentially decaying solutions consistent with the Meissner state. When $\chi' > 1$, one finds oscillatory solutions consistent with antiferromagnetic superconductivity.

There are two regions in the phase diagram of a magnetic superconductor where one can consider a type I–type II phase transition. Firstly at extremely high values of susceptibility (not shown in figure 2) the condition given by equation (49) must eventually be met so the material becomes an antiferromagnetic superconductor. Whether the material passes through the ferromagnetic phase or not depends on the material's κ-value. For antiferromagnetic superconductivity, there are equal numbers of fluxons and antifluxons in the material so the net flux density is zero and the material behaves macroscopically similarly to a type I material in the Meissner state. Secondly, when $\chi' \cong 1$, $\beta_A \to \infty$ which implies very large variations in the magnetic field which will eventually render the perturbation approach used in this paper invalid. Nevertheless, in this limit one can expect widely separated chains of fluxons leaving macroscopic regions which contain no fluxons and may lead to a type I–type II transition.

6. Comparison with the literature

The simplicity of the isotropic model considered in this paper cannot provide a complete description of complex materials. There are many material-dependent microscopic properties and magnetic interactions including spin-flip scattering, conduction electron polarization, the degree of non-locality and RKKY interactions [11, 13, 17, 18, 30, 32, 37–44] that have been considered in the literature within the G–L framework and could be required. We note that if superconductors are considered that are more complex than those in this paper, additional interactions must be written in terms of local parameters and $\boldsymbol{M}$. In a layered superconductor [45–49] or a material with superelectrons constrained to parts of the unit cell (which is almost inevitable in conventional superconductors with coexisting superconductivity and magnetism), the value of κ assigned to the parent material would be higher than that of the superconducting layer alone, since $(\partial \langle \boldsymbol{M}_{SC} \rangle / \partial \langle \boldsymbol{H}_{ext} \rangle)_{H_{ext} \approx H_{C2}}$ is averaged over the volume of the material rather than just the layer—hence one may expect non-hexagonal structures to occur at higher values of κ in layered superconductors. For example, although unconventional superconductivity has been suggested as the origin of the square flux-line lattice in Sr_2RuO_4, it has nearly two-dimensional metallic properties and a κ-value of only 2.6 [15, 50] (and incipient ferromagnetism [51]). We make the general observation that the non-hexagonal structure is well established experimentally in low-κ isotropic metallic materials [7, 9], in layered metallic [52] superconductors such as YNi_2B_2C [53] and in magnetic superconductors [14–16]. It also tends to occur at low temperatures, where one can expect to find strong paramagnetism consistent with the results of this work.

6.1. Type I–type II magnetic phase transition

The result

$$\frac{\partial\langle \boldsymbol{M}_{SC}\rangle}{\partial\langle \boldsymbol{H}_{ext}\rangle}_{H_{ext}\approx H_{C2}} = \frac{1}{3}$$

for metallic type II superconductors at low κ-values can be compared to the standard G–L result

$$\frac{\partial\langle \boldsymbol{M}_{SC}\rangle}{\partial\langle \boldsymbol{H}_{ext}\rangle}_{H_{ext}\approx H_{C2}} = \frac{1}{(2\kappa^2-1)\beta_A}$$

which approaches infinity as $\kappa \to 1/\sqrt{2}$. In figure 3, the magnetic properties of a cylindrical polycrystalline tantalum wire doped with nitrogen [21] are shown (converted to S.I. units). As the temperature decreases, κ increases and the material changes from type I to type II. The dashed lines show that $(\partial\langle \boldsymbol{M}_{SC}\rangle/\partial\langle \boldsymbol{H}_{ext}\rangle)_{H_{ext}\approx H_{C2}}$ is a weak function of κ close to the type I–type II phase transition. In particular, at 3.5 K although the material is almost type I, $(\partial\langle \boldsymbol{M}_{SC}\rangle/\partial\langle \boldsymbol{H}_{ext}\rangle)_{H_{ext}\approx H_{C2}}$ has the relatively low value of ∼1.7. Similarly low values (but less comprehensive magnetic data) are available for Nb [4] and V [5].

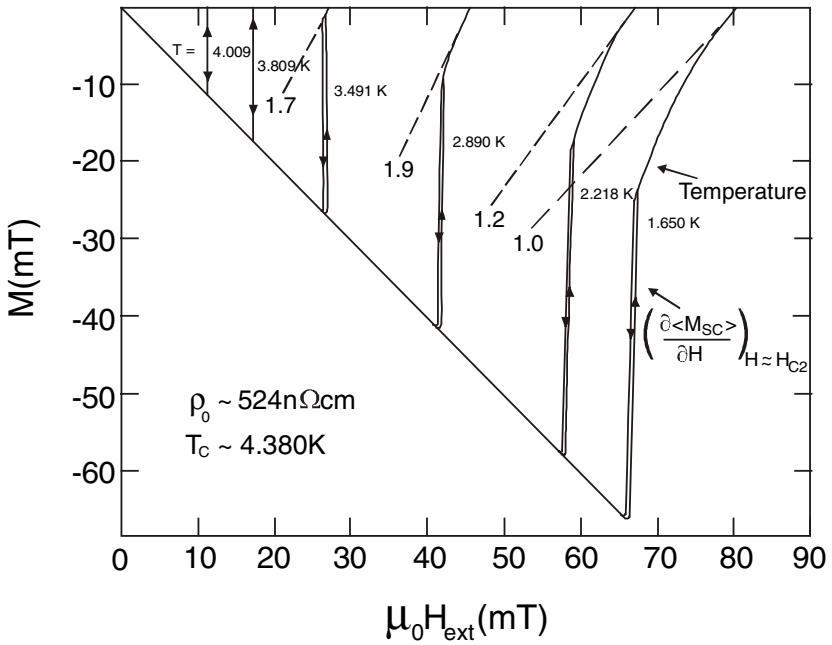

Figure 3. Highly reversible magnetization curves for a TaN wire as functions of field and temperature. The temperatures have been rounded to two significant figures. The dashed lines give values for $(\partial\langle \boldsymbol{M}_{SC}\rangle/\partial\langle \boldsymbol{H}_{ext}\rangle)_{H_{ext}\approx H_{C2}}$ at each temperature. Data from Auer and Ullmaier [21].

In figure 4 (upper panel), a type I–type II phase transition is shown for a spherical single crystal of the magnetic superconductor $ErRh_4B_4$ for the field applied along the $\boldsymbol{a}$-axis [23]. Crabtree *et al* [22] have highlighted the first-order transition by presenting data on a spherical crystal of $ErRh_4B_4$ in terms of the internal field (figure 4, lower panel). There is qualitative agreement with theory since the phase transition is not observed when the field is applied along the very weakly paramagnetic $\boldsymbol{c}$-axis, implying that the phase transition is driven by strong paramagnetism. This interpretation implies that at low temperatures,

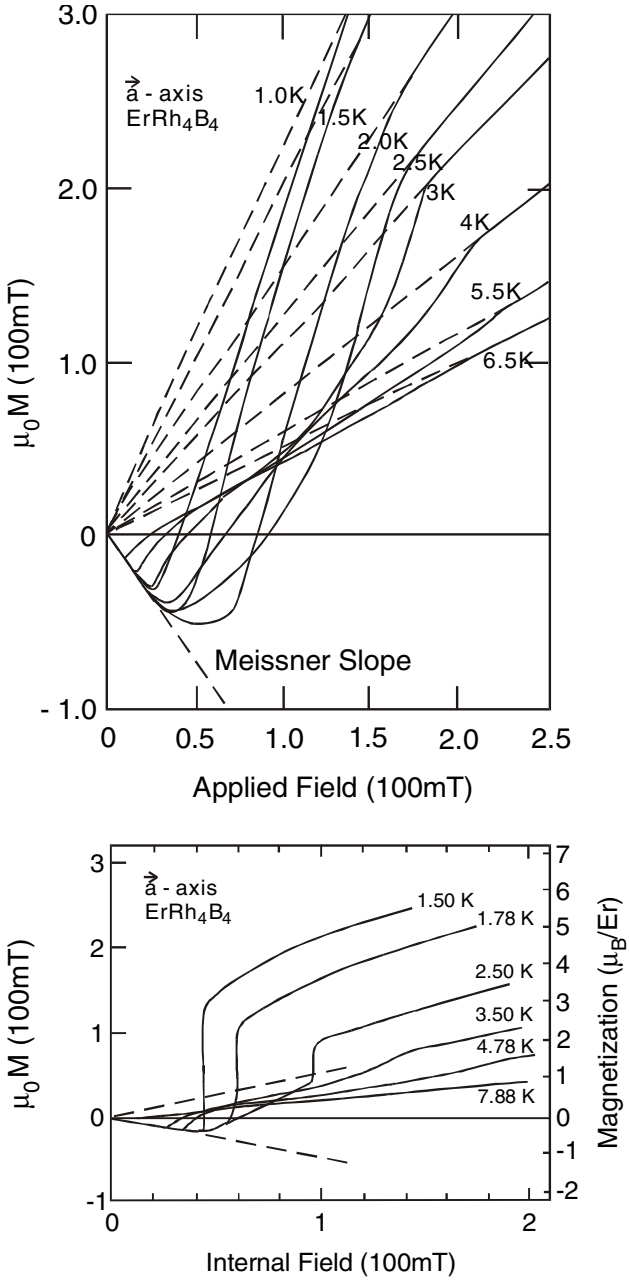

Figure 4. Magnetization curves for spherical single crystals of $ErRh_4B_4$ when the magnetic field is applied along the a-axis. Upper panel: the initial magnetic response versus applied field. Data from Behroozi *et al* [23]. Lower panel: $\mu_0 M$ versus internal field. Data from Crabtree *et al* [22].

the low-magnetic-field phase is antiferromagnetic superconductivity. We also note that the appearance of a spontaneous magnetic field in zero applied field at temperatures well below T_C, for example in the magnetic superconductor UPt_3, may be explained by antiferromagnetic superconductivity [54].

6.2. Transport properties—re-entrant superconductivity

Finally, we discuss the evidence for the assertion that as magnetic superconductors become strongly paramagnetic they tend to show re-entrant superconductivity. Although the thermodynamic arguments in this paper cannot explain resistance versus temperature data, we discuss whether the change in the connectivity of the fluxons at $\chi' \cong 1$ plays a role. The work of Kleiner *et al* [36] shows that apart from the hexagonal structure for which there is a unique value of β_A, in general more than one structure can have the same value of β_A and hence the lowest Gibbs energy. For example, a square structure and a rhombohedral structure (where the ratio of the diagonals is $\sim$2.3) both have a value of β_A equal to 1.18 [36]. Clearly any anisotropy or flux pinning may lift the degeneracy of these different structures. In the case of very high values of β_A(Max), there may be well-separated chains of closely spaced fluxons that extend across the entire sample. The wavefunction will be strongly depressed in these chains when the normal cores of the fluxons overlap, giving barriers of weakly superconducting material. This would be similar to type I superconductors in the intermediate state [7] where one can observe resistance when there is no percolative path around fluxon barriers. The resistance may either be due to flux flow because of weak pinning or dissipation as the local depairing current is reached in the barriers. Hence when $\chi' \cong 1$, the material may become resistive.

The classes of materials that are considered are the Chevrel phase materials [33] and the nickel–boron carbides [34]. The materials show coexistence of long-range magnetic ordering and superconductivity with magnetic ordering temperatures that are relatively low. In general, the magnetic ions that can be incorporated in these materials have measured Bohr magneton values that are similar to theoretical values for free ions [55, 56]. This is consistent with band-structure calculations which show there is very little overlap between the conduction electrons and magnetic ions [32]. For example, in the Chevrel phase materials, the Curie temperatures are in the range of 0.5–2 K, which suggests that the exchange interaction is relatively weak and dipolar interactions are important—as assumed in section 3.

Magnetic properties are considered first. The nickel–boron carbide materials are strongly anisotropic. For example, in $DyNi_2B_2C$, when $\boldsymbol{H}_{ext} \parallel c$-axis and $\boldsymbol{H}_{ext} \perp c$-axis, the Curie–Weiss temperature is -25 K and +82 K respectively [57, 58]. Even in the Chevrel phase materials, which have almost cubic structure and almost isotropic properties, the precise composition affects the crystal field and the temperature dependence of the differential susceptibility. In table 1, values of the Curie–Weiss temperature (θ_{CW}) and the effective Bohr magneton number (p_{eff}) for strongly magnetic Chevrel phase (rare-earth–Mo_6S_8) and nickel–boron carbide superconductors are presented. The values in table 1 are for bulk poly-crystalline samples so they are angular averages [56, 59]. The values of θ_{CW} and p_{eff} for the Chevrel phase materials were calculated from differential susceptibility measurements in the temperature range below 15 K, except for the $GdMo_6S_8$ where the values have been determined for $T < 300$ K. The nickel–boron carbide values are from differential susceptibility data below 100 K. The uncertainty in θ_{CW} is typically $\sim$3 K for the nickel–boron carbides and $\sim$1 K for the Chevrel phase materials. The values of p_{eff} are similar to theoretical calculations for isolated ion values [27]. An estimate for the temperature ($T_{\chi'=1}$) at which χ' extrapolates to 1 can be found by using the Curie–Weiss law

$$\chi' = C/(T + \theta_{CW})$$

where $C = 2.6p_{eff}^2/V$ (Å^3) and V (Å^3) is the volume of the atomic formula unit cell in Å^3 (i.e. $T_{\chi'=1} = C - \theta_{CW}$). Clearly there are concerns when using the isotropic Curie–Weiss law to describe such complex materials; for example, magnetic ordering is ignored. Nevertheless we suggest that $T_{\chi'=1}$ gives a reasonable first approximation for the temperature at $\chi' \cong 1$.

Table 1. The Curie–Weiss temperature (θ_{CW}), the effective Bohr magneton number (p_{eff}, dimensionless), the Curie constant (C), the temperature at which the differential susceptibility extrapolates to 1 ($T_{\chi'=1}$) and the temperature for the re-entrant resistive behaviour (T_ρ) for strongly magnetic nickel–boron carbide [56] and Chevrel phase superconductors [32, 59, 60]. $T_{\chi'=1}$ is set to zero when calculated to be negative. For $TbNi_2B_2C$ and $DyNi_2B_2C$, detailed measurements are not available for the superconducting state below 2 K.

	Nickel–boron carbides					Chevrel phases				
	Tb	Dy	Ho	Er	Tm	Gd	Tb	Dy	Ho	Er
θ_{CW}/K	−10.2	−9.8	−1.5	−2.2	10.8	+1	−1.1	−0.15	+0.35	+0.45
p_{eff}	11.1	10.4	9.8	7.7	9.9	7.5	9.59	10.4	10.60	9.53
C/K	2.5	2.2	1.9	1.2	2.0	0.53	0.87	1.02	1.06	0.86
$T_{\chi'=1}$/K	12.7	12.0	3.4	3.4	0	0	1.97	1.17	0.71	0.41
T_ρ/K	—	—	6.0	6.0	2.6	0.95	1.0	0.6	0.75	0.6

In typical re-entrant resistive behaviour, the resistance first drops at the superconducting transition. As the temperature decreases further, the resistance passes through a minimum, and then increases showing the re-entrant resistive behaviour followed by re-entrant superconductivity [32, 56, 60]. The mechanism causing the resistance must both switch on over a limited temperature range and then switch off again at lower temperatures. To simplify the explanation, typical data from the literature are shown in figure 5 for $Gd_{1.2}Mo_6S_8$. We have chosen to characterize the re-entrant behaviour by the temperature (T_ρ) at which the resistance passes through the minimum. In table 1, values of T_ρ for strongly magnetic Chevrel phase (rare-earth–Mo_6S_8) and nickel–boron carbide superconductors are presented [56, 59].

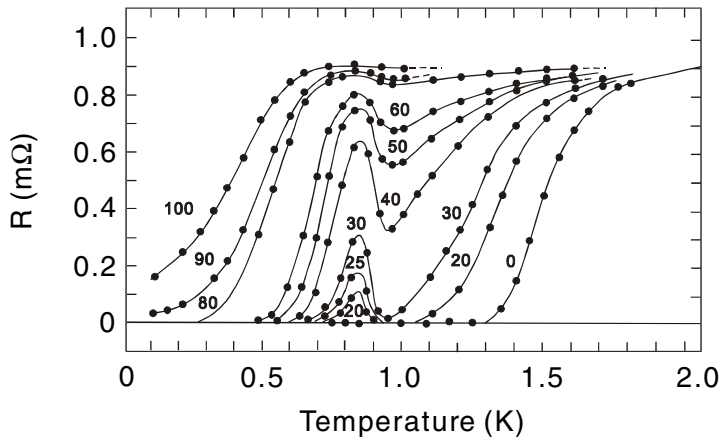

Figure 5. The resistance of $Gd_{1.2}Mo_6S_8$ as a function of temperature and dc magnetic field. Clear re-entrant behaviour is observed. Data from the textbook edited by Maple and Fischer [32].

Comparing the values of $T_{\chi'=1}$ and T_ρ in table 1, all the Chevrel phase materials for which θ_{CW} and p_{eff} have been measured for $T < 15$ K (i.e. except $GdMo_6S_8$) show re-entrant behaviour at about 1 K. Re-entrant resistance preferentially occurs when the material becomes strongly paramagnetic, whether the exchange interaction is ferromagnetic or antiferromagnetic (i.e. θ_{CW} negative or positive). The re-entrant behaviour of $TmNi_2B_2C$ is at only 2.6 K although p_{eff} is high. In the $HoNi_2B_2C$ and $ErNi_2B_2C$, there is reasonably good agreement between the values of $T_{\chi'=1}$ and T_ρ [56]. For $TbNi_2B_2C$ and $DyNi_2B_2C$, neither

the differential susceptibility nor possible re-entrant resistance has yet been investigated in the superconducting state below 2 K.

In the light of the complexity of the Chevrel phase and (particularly) the nickel–boron carbide superconductors, the simplicity of the isotropic theory and the limited data available, we conclude that there is some evidence for a correlation between the re-entrant resistance and magnetic superconductors becoming strongly paramagnetic (i.e. $\chi' \gtrsim 1$). Re-entrant resistive behaviour has only otherwise been observed at low temperatures ($\sim$1 K) in materials such as the rhodium borides that include rare-earth (strongly paramagnetic) ions [61]. We are not aware of any established explanation in the literature for the correlation of strong paramagnetism in magnetic superconductors and re-entrant resistivity.

7. Concluding comments

Results presented in this paper are consistent with the magnetic properties predicted for metallic superconductors using standard analysis when $\kappa^2 \gg 1$. For low-κ materials, new equilibrium properties have been found which are not consistent with the standard description [31]. In particular we propose there is a special class of low-κ superconductors with a non-hexagonal flux-line lattice for which $\langle M_{SC} \rangle$ is independent of κ. When materials that are strongly paramagnetic in the normal state become superconducting, a ferromagnetic contribution from the superelectrons can be produced in high magnetic fields and an antiferromagnetic one in low fields. Our long-standing interest in flux pinning in magnetic and metallic superconductors was the original motivation for this work. Reliable expressions for the Gibbs energy are a prerequisite for addressing the long-standing issues of calculating elastic constants for the flux-line lattice [62], the strength of magnetic and non-magnetic pinning sites [63] and reliable solutions for the so-called 'grand summation' of pinning forces [64]. The generalized G–L theory will impact on these areas and others that are of interest to the superconductivity community.

Acknowledgments

DPH thanks the EPSRC for his Advanced Fellowship, P Russell for help producing the figures and Amanda, Emily, Peter and Alexander for their support.

References

[1] Ginzburg V L and Landau L D 1957 On the theory of superconductivity *Zh. Eksp. Teor. Fiz.* **20** 1064
[2] Gorkov L P 1958 On the energy spectrum of superconductors *Sov. Phys.–JETP* **37** 505
[3] Abrikosov A A 1957 On the magnetic properties of superconductors of the second group *Sov. Phys.–JETP* **5** 1174
[4] Finnemore D K, Stromberg T F and Swenson C A 1966 Superconducting properties of high-purity niobium *Phys. Rev.* **149** 231
[5] Radebaugh R and Keesom P H 1966 Low-temperature thermodynamic properties of vanadium: II. Mixed state *Phys. Rev.* **149** 217
[6] Kumpf U 1971 *Phys. Status Solidi* b **44** 829
[7] Huebner R P 1979 *Magnetic Flux Structures in Superconductors* (New York: Springer)
[8] Tinkham M 1996 *Introduction to Superconductivity* 2nd edn (Singapore: McGraw-Hill)
[9] Obst B 1969 Rectangular flux line lattice in type II superconductors *Phys. Lett.* A **28** 662
[10] Obst B 1971 Anisotropie in kubischen Supraleitern *Phys. Status Solidi* b **45** 467
[11] Ullmaier H, Zeller R and Dederichs P H 1973 Correlation between vortex lattice and crystal lattice in type-II superconductors due to elastic interaction *Phys. Lett.* A **44** 331

[12] Takanaka K 1973 Correlation between flux-line lattice and crystal axis in a mixed state of superconductors *Prog. Theor. Phys.* **50** 365
[13] Teichler V H 1973 Anisotropy of the asymptotic structure of isolated flux-lines and plane phase boundaries in cubic superconductors *Phil. Mag.* **31** 789
[14] Eskilden M R *et al* 1998 Intertwined symmetry of the magnetic modulation and the flux-line-lattice in the superconducting state of $TmNi_2B_2C$ *Nature* **393** 242
[15] Riseman T M *et al* 1998 Observation of a square flux-line lattice in the unconventional superconductor Sr_2RuO_4 *Nature* **396** 242
[16] Yaron U *et al* 1996 Microscopic coexistence of magnetism and superconductivity in $ErNi_2B_2C$ *Nature* **382** 236
[17] Kogan V G *et al* 1997 Vortex lattices in cubic superconductors *Phys. Rev. Lett.* **79** 741
[18] Berlinsky A J *et al* 1995 Ginzburg–Landau theory of vortices in d-wave superconductors *Phys. Rev. Lett.* **75** 2200
[19] Agterberg D F 1998 Vortex lattice structures of Sr_2RuO_4 *Phys. Rev. Lett.* **80** 5184
[20] Hampshire D P 1998 Ferromagnetic and antiferromagnetic superconductivity *Physica* C **304** 1
[21] Auer J and Ullmaier H 1973 Magnetic behaviour of type II superconductors with small Ginzburg–Landau parameters *Phys. Rev.* B **7** 136
[22] Crabtree G W *et al* 1986 Tricritical behaviour in the ferromagnetic superconductor $ErRh_4B_4$ *J. Magn. Magn. Mater.* **54** 703
[23] Behroozi F *et al* 1983 Observation of the first-order phase transition in single-crystal of $ErRh_4B_4$ at H_{C2} *Phys. Rev.* B **27** 6849
[24] de Gennes P 1989 *Superconductivity of Metals and Alloys* (Redwood City, CA: Addison-Wesley)
[25] Landau E M and Lifshitz I M 1960 *Electrodynamics of Continuous Media* vol 8 (Oxford: Pergamon)
[26] Campbell A M 2001 *Magnetic Properties of Superconductors* (Bristol: Institute of Physics Publishing) at press
[27] O'Handley R C 2000 *Modern Magnetic Materials* (New York: Wiley)
[28] Tilley D R and Tilley J 1990 *Superfluidity and Superconductivity* 3rd edn (Bristol: Institute of Physics Publishing)
[29] Gray K E 1983 Ginzburg–Landau equations, interphase surface energy, and the intermediate state of superconductors with a paramagnetic normal state *Phys. Rev.* B **27** 4157
[30] Pippard A B 1953 An experimental and theoretical study of the relation between magnetic field and current in a superconductor *Proc. R. Soc.* A **216** 547
[31] Brandt E H 1997 Precision Ginzburg–Landau solution of ideal vortex lattices for any induction and symmetry *Phys. Rev. Lett.* **78** 2208
[32] Maple M B and Fischer O (ed) 1982 *Superconductivity and Magnetism (Superconductivity in Ternary Compounds vol 2)* (Berlin: Springer)
[33] Chevrel R, Sergent M and Prigent J 1971 Sur de nouvelles phases sulfurees ternaires du molybdene *J. Solid State Chem.* **3** 515
[34] Cava R J *et al* 1994 Superconductivity in the quaternary intermetallic compounds $LnNi_2B_2C$ *Nature* **367** 252
[35] Ginzburg V L 1957 Ferromagnetic superconductors *Sov. Phys.–JETP* **4** 153
[36] Kleiner W H, Roth L M and Autler S H 1964 Bulk solution of Ginzburg–Landau equations for type II superconductors: upper critical field region *Phys. Rev.* **133** A1226
[37] Takanaka K 1975 Magnetic properties of superconductors with uniaxial symmetry *Phys. Status Solidi* b **68** 623
[38] Grobmann S and Wissel Ch 1972 Phase transition of first order in superconductors at H_{C1} *Z. Phys.* **252** 74
[39] Kramer L 1966 Thermodynamical behaviour of type-II superconductors with small kappa near the lower critical field *Phys. Lett.* **23** 619
[40] Kuper C G, Revzen M and Ron A 1980 Ferromagnetic superconductors: a vortex phase in ternary rare-earth compounds *Phys. Rev. Lett.* **44** 1545
[41] Matsumoto H, Umezawa H and Tachiki M 1979 A new phase in magnetic superconductors *Solid State Commun.* **31** 157
[42] Ferrell R A, Bhattacharjee J K and Bagchi A 1979 Effect of nonlocality on the spin correlations in ferromagnetic superconductors *Phys. Rev. Lett.* **43** 154
[43] Blount E L and Varma C M 1979 Electromagnetic effects near the superconductor-to-ferromagnetic transition *Phys. Rev. Lett.* **42** 1079
[44] Greenside H S, Blount E I and Varma C M 1981 Possible coexisting superconducting and magnetic states *Phys. Rev. Lett.* **46** 49
[45] Tachiki M and Takahashi S 1989 Anisotropy of critical current in layered superconductors *Solid State Commun.* **72** 1083
[46] Klemm R A, Luther A and Beasley M R 1975 Theory of the upper critical field in layered superconductors *Phys. Rev.* B **12** 877
[47] Prober D E, Schwall R E and Beasley M R 1980 Upper critical fields and reduced dimensionality of the

superconducting layered compounds *Phys. Rev.* B **21** 2717
[48] Clem J R 1991 Two-dimensional vortices in a stack of thin superconducting films: a model for high-temperature superconducting multilayers *Phys. Rev.* B **43** 7837
[49] Lawrence W E and Doniach S 1971 *Proc. 12th Int. Conf. on Low Temperature Physics (Kyoto)* unpublished
[50] Luke G M *et al* 1998 Time-reversal symmetry-breaking superconductivity in Sr_2RuO_4 *Nature* **394** 558
[51] Maeno Y, Rice T M and Sigrist M 2001 The intriguing superconductivity of strontium ruthenate *Phys. World* (1) 42
[52] Song K J *et al* 1999 Nonlocal current–field relation and the vortex-state magnetic properties of YNi_2B_2C *Phys. Rev.* B **59** R6620
[53] Sakata H *et al* 2000 Imaging of a vortex transition in YNi_2B_2C by scanning tunneling spectroscopy *Phys. Rev. Lett.* **84** 1583
[54] Luke G M *et al* 1993 Muon spin relaxation in UPt_3 *Phys. Rev. Lett.* **71** 1466
[55] Fischer O 1978 Chevrel phases: superconducting and normal state properties *Appl. Phys.* **16** 1
[56] Eisaki H *et al* 1994 Competition between magnetism and superconductivity in rare-earth nickel boron carbides *Phys. Rev.* B **50** 647
[57] Cho B K, Canfield P C and Johnston D C 1995 Onset of superconductivity in the antiferromagnetically ordered state of single-crystal $DyNi_2B_2C$ *Phys. Rev.* B **52** R3844
[58] Peng Z Q, Krug K and Winzer K 1998 Large hysteresis effect and reentrant behaviour in $DyNi_2B_2C$ *Phys. Rev.* B **57** R8123
[59] Pellizone M *et al* 1977 Magnetic susceptibility of $(\text{Rare Earth})_x Mo_6S_8$ *J. Low Temp. Phys.* **29** 453
[60] Ishikawa M and Fischer O 1977 Magnetic ordering in the superconducting state of rare earth molybdenum sulphides, $(RE)_{1.2}Mo_6S_8$ (RE = Tb, Dy, and Er) *Solid State Commun.* **24** 747
[61] Bulaevskii L N *et al* 1985 Coexistence of superconductivity and magnetism; theoretical predictions and experimental results *Adv. Phys.* **34** 175
[62] Brandt E H 1977 Elastic energy of the vortex state in type II superconductors—high inductions *J. Low Temp. Phys.* **26** 709
[63] Alden T H and Livingston J D 1966 Ferromagnetic particles in a type-II superconductor *J. Appl. Phys.* **37** 3551
[64] Campbell A M and Evetts J E 1972 Flux vortices and transport currents in type II superconductors *Adv. Phys.* **21** 395